Determining Bulk Factors for Three Subsoils Used in Forest Engineering in Slovenia

Jan Mihelič, Robert Robek, Milan Kobal

Abstract

In Slovenia, torrent areas and forest roads are being regulated and built mostly in steep, erosion-prone areas. In addition to the geometry of extrapolated works, calculating bulk factors is key for estimating haulage masses. We have determined bulk factors for compact carbonate rock, mixed soil, and carbonate deposits. Each construction site was recorded with an unmanned aerial vehicle (UAV) before the excavation and after every 4±2 m^3 of excavated material. The average point cloud density was 9535 points/m^2. We processed the point clouds from each construction site and determined the difference in volume between the volume of excavated area and the volume of deposited material. The average bulk factor for compact carbonate rock is 1.42, 1.20 for mixed soil and 1.15 for carbonate deposits (calculated for fully loaded eight-wheeled truck). The calculated bulk factors for soils and carbonate deposits match with the already established values, while the factor for compact rock is 20% lower than the factor currently in use by the Slovenian forest engineers.

Keywords: excavation, embankment, photogrammetry, dense point cloud, UAV, volume calculations

1. Introduction

There is considerable uncertainty regarding earthwork calculation in forest road construction and management of torrent areas. To predict the appropriate amount of excavated and backfill material, bulk and shrink factors are used, representing the ratio of bank (in-situ) to loose volume – the bulk factor – or the ratio of bank to shrinked material volume – the shrink factor (Strgar 2004). Knowing the bulk and the shrink factor values for actual materials at project level facilitates the investment process (Chopra 1999).

Most forest design engineers use the above factors based on their own experiences, past information, or construction handbooks. Factor values differ by water content, material density or unit weight and soil type (Burch 1997). Several aspects affect the determination of bulk and shrink factors: type of rock or lithology, in-situ porosity which influences the in-situ density, grain size and shape, rock strength and mass structure, fall height of individual blocks, vibratory compaction, and vertical stress. For the latter, Ofoegbu et al. (2008) described a negative non-linear relationship between the bulk factor and overburden stress.

The bulk factor can be determined in a variety of ways. For granular materials, it can be calculated by comparing the amount of loose material needed to fill a wooden box of volume 0.028–0.057 m^3 (1–2 ft^3) against the original excavated volume (Peele 1961). For larger amounts of material – such as excavation and backfill piles – one of the geometric approaches must be used (Church 1981). For compact materials, bulk factors can be determined by comparing the densities of crushed and compact rock by using samples or determining the bulk density in drill holes. For representative factor values, it is necessary to make several volume and mass measurements (Telford et al. 1976).

An alternative way of determining the bulk or shrink factor is to compare the volumes of crushed material with the in-situ volume of bank material. For volume change monitoring, precision laser and photo scanners attached to different platforms can be used. Unlike the conventional survey approaches (such as the use of a total station), these instruments can generate a dense grid of laser beams or a large number of high-quality photos which can be used to create a 3D point cloud (Kobal et al. 2014). This is a base for generating precise digital surface models; based on the

difference between two digital surface models, we can calculate pile volumes and thus determine the bulk factors. Such modern approaches are common in different forestry industries – there are many research articles associated with modern techniques of forest wood production, such as stereovision system for the in-field estimation of tree parameters (Costa et al. 2018), virtual environment-assisted teleoperation (Westerberg et al. 2013) that, like in our research, uses image sensors to create 3D surface model.

In construction engineering, where changes in the amount and the shape of material are common, the use of remote data sensing with unmanned aerial vehicles (UAV) is rapidly increasing. UAVs differ in shape and dimension: different types of sensors can be mounted according to the intended use (from multispectral, RGB cameras to laser scanners). One of the disciplines that recently made significant progress in this area is close range photogrammetry. It is the science of obtaining reliable metric information, usually from two or more photos from the same area, resulting in three-dimensional surface models (Schenk 2005).

There are many studies describing the use of photogrammetry for different purposes, but only few of them compare the accuracy of photogrammetric models obtained with this method. When it comes to volume calculations, the findings mostly confirm the applicability of the photogrammetric method. The authors observe that the calculation of volume by this method is faster, more accurate and better from the point of view of cost savings, compared to volume calculation by conventional methods (Yilmaz 2010, Arango and Morales 2015). Hugenholtz et al. (2015) found that the vertical accuracy of a point cloud obtained by the photogrammetric method using an UAV with the correct use of ground control points is comparable, if not better than airborne laser scanning, but less accurate than terrestrial laser scanning. The authors concluded that calculating the volume using an UAV makes the most sense in projects of size between 0.05 and 30 km^2. For smaller areas, volume calculations are more appropriate using a total station, a terrestrial scanner, and a GNSS receiver; for areas larger than 30 km^2, volume calculations make the most sense using airborne laser scanning.

Sanz-Ablanedo et al. (2018) studied the influence of the number of ground control points on the accuracy of cloud point georeferencing and determined that the achieved horizontal accuracy in the raster cell size range was achieved with 2.5 to 3 ground control points per 100 photos taken. Horizontal accuracy does not improve significantly with the use of more than 3

control points per 100 photos, while vertical accuracy had steadily improved until the use of 4 ground control points per 100 photos.

The aim of the study was to determine the bulk factors for three common subsoils often used in forest construction and torrential areas: carbonate deposits, mixed soil, and compact carbonate rocks. The focus of the study was to examine the differences in bulk factors between these materials regarding the considered volume of material. We have defined two research hypothesis:

⇒ bulking factors differ over three common subsoils

⇒ bulking factors from literature differ from our calculated factors.

2. Materials and Methods

Field measurements were taken at three construction sites on the Jelovica plateau (northwestern Slovenia), where the construction of forest roads took place between June and August 2019. The site was selected according to the geological basis present there – we analysed:

⇒ mixed soil – construction site Kopiša

⇒ compact carbonate rock – construction site Kamnica

⇒ carbonate deposits – construction site Pašni vrh.

2.1 Used Equipment and Machinery

In the study, we used:

⇒ DELL XPS 15 (9570) i9-8950HK, 32GB RAM, SSD 1TB, GTX1050Ti

⇒ DJI Mavic 2 PRO drone

⇒ Leica Viva TS12 Total Station

⇒ Leica Z Rover GNSS receiver consisting of a Leica Zeno 20 GNSS receiver with an external Geodetic Antenna Leica AS10 GNSS

⇒ 7.5 t Takeuchi excavator with a 0.3 m^3 loading shovel on construction sites 2 and 3

⇒ 23 t CAT excavator and 3 t hydraulic hammer on site 1. We used a 1 m^3 loading shovel to load crushed compact rock on the truck.

2.2 Field Data Capture

The construction site 1 with the compact carbonate rock (Kamnica) was divided into 6 plots. Before the UAV recordings began, the excavator operator removed the topsoil and the weathered layer in all

Fig. 1 Total station (a) on construction site 1 (plot 6), GNSS receiver (b), and a UAV (c)

the plots with a loading shovel until the compact base was reached; from there, we continued with the hydraulic hammer. The same working conditions were established at all Kamnica plots: the same hammer power, the maximum grain size of 30 cm, and side placement of the machine during hammering. During the excavation process, we performed an image based sieving analysis with Split Desktop programme from Split Engineering company LLC (2019). After the hammering was finished, the excavator operator placed the loading shovel on the excavator and then loaded and drove each pile to the turning zone separately, where they were finally measured with the total station.

The construction sites 2 (Kopiša) and 3 (Pašni vrh) were divided into 4 plots. Before the UAV recordings began, the excavator operator removed the stumps and the top layer of vegetation in all plots with a loading shovel, until mineral soil was reached. The excavator operator loaded the material into the truck as he went along.

We placed 4 to 5 ground control points (round black targets with a diameter of 30 cm) on each site, distributing them evenly across the plots. The coordinates of the points were measured by the arithmetic mean of three 10-second independent measurements using the GNSS-RTK method. At the sites, where the coordinates of the ground control points could not be reliably recorded with the GNSS receiver due to the lack of signal, the coordinates were determined by the total station. For different methodology comparison, each pile at the construction site 1 (Kamnica) was measured with the total station (Fig. 1).

The UAV recordings (Fig. 1) were performed in three consecutive arrays for every 4 ± 2 m^3 of excavated material. The UAV was operated using the Pix4Dcapture mobile application, designed for flight planning and monitoring, installed on the Android operating system. All the photos taken were stored on a microSD card with 64 GB of memory.

The UAV recordings were performed on individual plots under the same recording conditions. Therefore, the same flight trajectories and the same number of photos with the spatial resolution of less than 1 cm were used in all recordings. We flew at an altitude between 20 and 27 m with an 85% photo overlap, using a double grid mission optimal for creating 3D models. The speed of the drone during the flight was 2 m/s. A total of 3605 photos were taken (Table 1).

Table 1 The main characteristics on individual construction sites

	Kamnica	Kopiša	Pašni vrh
Excavator	20 t excavator with a 3 t hammer and an 1 m^3 loading shovel	7.5 t excavator with an 0.3 m^3 loading shovel	7.5 t excavator with an 0.3 m^3 loading shovel
No. of plots	6	4	4
No. of flights	19	11	12
No. of images taken	1772	682	1151

2.3 Data Processing

First, we performed the bundle adjustment in the 3Dsurvey 2.9.1 program (3Dsurvey 2019) to align the image blocks, which resulted in a sparse point cloud. We selected the coordinate system of the imported data (WGS 1984) and the coordinate system in which we exported point clouds and digital surface models (D96). After aligning the image blocks, we entered the data from ground control points and created a georeferenced point cloud. The georeferencing accuracy was checked for each point cloud by calculating the root mean square error *RMSE*. In total, 43 dense point clouds were created (Fig. 2).

Digital surface models (DSM) with a grid cell size of 0.02 m were produced for each site. For information on the initial state, we used a digital surface model created with data from an overflight taken before the construction work was carried out. The volume of the excavated and deposited material was calculated as the difference in DSM before construction work and DSM after each subsequent recording. In total, 43 digital surface models were created and 80 volume calculations were carried out.

The bulk factors for selected materials were calculated using the equation below (Chopra 1999), where the volume was calculated on the basis of the methods described above.

$$BF = \frac{V_L - V_E}{V_E} \qquad (1)$$

Where:

BF bulk factor

V_E bank volume (in-situ)

V_L loose volume of material.

The bulk factor is influenced significantly by the size and shape of grains, which is why we have determined grain fragmentation for each plot of deferred material on construction site 1. We used the Split Desktop programme (Split Engineering LLC (2019)) and a smartphone with the Split Camera application to take pictures of the piles.

The statistical processing was carried out using the R Studio program (RStudio Team 2015). The differences between the arithmetic mean were checked by the one-way analysis of variance (one-way ANOVA). The dependence of bulk factors and loose material volume was described with linear regression. We used a logarithmic transformation.

It is important to know the differences between the terms bulk factor and bulk percentage. Factors are applied to earthwork calculations and are used as conversions between different volumetric states. Bulk values refer to the potential of a material to expand in volume. This potential usually comes in the form of a
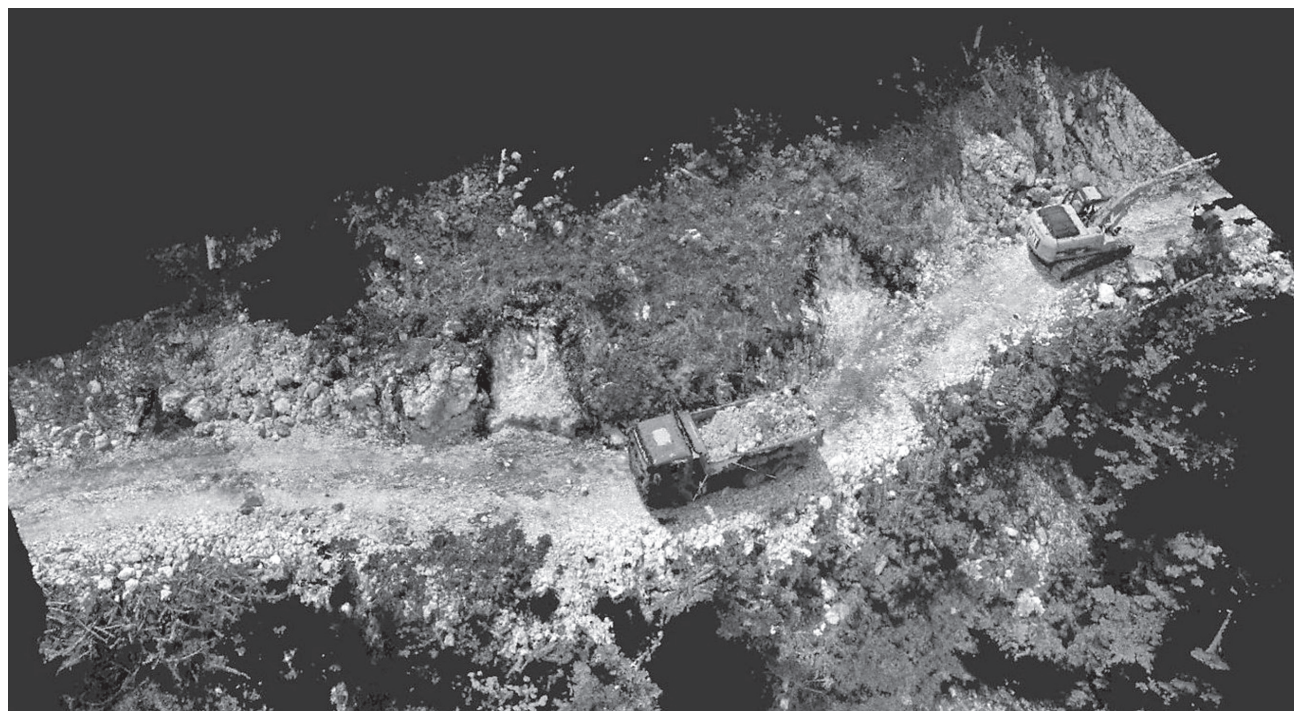

Fig. 2 Dense point cloud from plots 3 and 4 on construction site 1

Table 2 Point cloud characteristics on analysed construction sites

Construction site	Number of point clouds	Average time for creating a sparse point cloud, min:s	Average time for creating a dense point cloud, min:s	Average density of point clouds, points/m^2	$RMSE$ – average of all point clouds, m
1 – Kamnica	19	23:18	81:04	9949	0.008
2 – Kopiša	11	15:03	58:20	13,106	0.009
3 – Pašni vrh	13	18:55	66:13	5550	0.007

percentage which can be converted to a factor for use in earthwork calculations (Crooks 2013). In our research, we described the bulk potential with percentages, except for the end result where we provided the values in factors.

3. Results

3.1 Point Cloud Establishment and Georeferencing Precision

The average time needed for the creation of a sparse point cloud ranged from 15 minutes and 33 seconds (construction site 2) to 23 minutes and 18 seconds (construction site 1). The average time required for the creation of a dense point cloud ranged from 58 minutes and 20 seconds (construction site 2) to 81 minutes and 4 seconds (construction site 1). The average time for the creation of point cloud on construction site 3 ranged from 18 minutes and 55 seconds (sparse point cloud) to 66 minutes and 13 seconds

(dense point cloud). In total, it took 64 hours and 44 minutes to process all the point clouds. The average density of the point clouds was 9535 points/m^2 and the corresponding average georeferencing precision ($RMSE$) was 0.008 m (Table 2 and Table 3).

3.2 Material Fragmentation

Image-based sieving analysis revealed that, in every plot at construction site 1, the maximal grain was less than 30 cm in diameter. In average, 50% of the grains were smaller than 10 cm and 25% of the grains were smaller than 3 cm in diameter. The carbonate bedrock in plots 5 and 6 visually indicated a more fractured and porous material; their sieving curves (Fig. 3), however, did not differ significantly from the other plots.

3.3 Bulk Factors

The calculated bulk percentages among analysed materials differ significantly ($p<0.001$). Taking into consideration all piles, the largest average bulk was

Table 3 Point cloud georeferencing statistics

| Construction site	Plot	No. of point clouds	No. of photos per cloud	No. of targets	$RMSE_x$, m	$RMSE_y$, m	$RMSE_z$, m	$RMSE_{xyz}$, m
1 – Kamnica	1 and 2	5	84	5	0.004	0.002	0.009	0.005
	3 and 4	4	67	5	0.012	0.003	0.020	0.012
	5 and 6	6	94	5	0.004	0.003	0.010	0.006
2 – Kopiša	1	3	62	5	0.006	0.008	0.015	0.009
	2	2	62	5	0.008	0.009	0.020	0.012
	3	2	62	5	0.008	0.010	0.017	0.012
	4	2	62	5	0.003	0.002	0.009	0.005
3 – Pašni vrh	1	3	80	4	0.003	0.010	0.015	0.003
	2	3	80	4	0.005	0.008	0.013	0.009
	3	3	80	4	0.003	0.008	0.011	0.007
	4	3	80	4	0.005	0.006	0.009	0.007
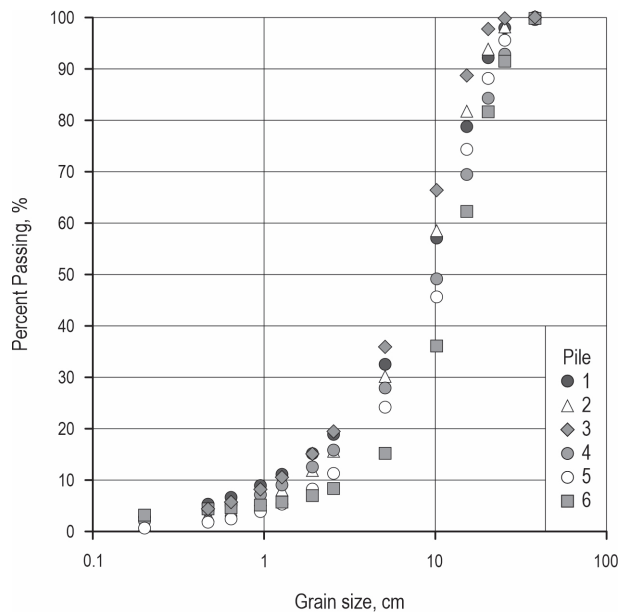
Fig. 3 Image-based sieving curves for compact carbonate material on construction site 1. X-axis is log transformed, where x means the logarithm to base 10

found for compact carbonate rock (46.5%), followed by mixed soil (25.7%), while the smallest average bulk was found for carbonate deposits (Fig. 4, Table 4).

The bulk percentage decreases by increasing the volume of loose material (*p*<0.01; Fig. 5). Statistical parameters are shown in Table 5.
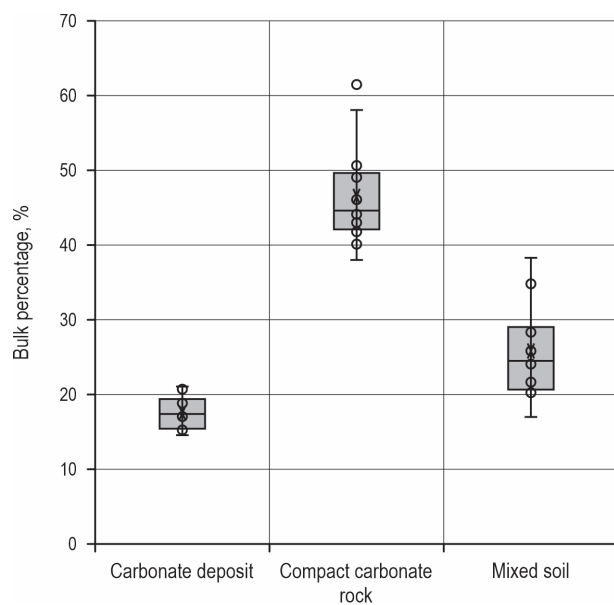
Table 4 Statistical parameters of boxplots

	n	*Mean*	*SD*	*SE*	*Median*
Carbonate deposits	12	17.48	2.19	0.63	17.41
Compact carbonate rock	16	46.50	6.32	1.58	44.60
Mixed soil	12	25.70	6.16	1.78	24.46

Table 5 Statistical parameters of regression

	Equation	n	R^2	P
Compact carbonate rock	$E = 68.62 - 12.41 \times \log(VL)$	16	0.66	$p < 0.001$
Mixed soil	$E = 54.09 - 13.73 \times \log(VL)$	12	0.63	$p = 0.0012$
Carbonate deposits	$E = 25.18 - 4.52 \times \log(VL)$	12	0.77	$p < 0.001$

In forest construction engineering, we are interested in the bulk factor for larger quantities of material, i.e. in the size class of one truck, which is why we have given the final value of the factors from the average value of the finished piles. Considering Fig. 5 for 9 m³ of scattered material, the mean bulk factor for compact carbonate rock is 1.42 (s.e. 1.1), 1.20 (s.e. 1.5) for mixed soil, and 1.15 for carbonate deposits (s.e. 0.5).
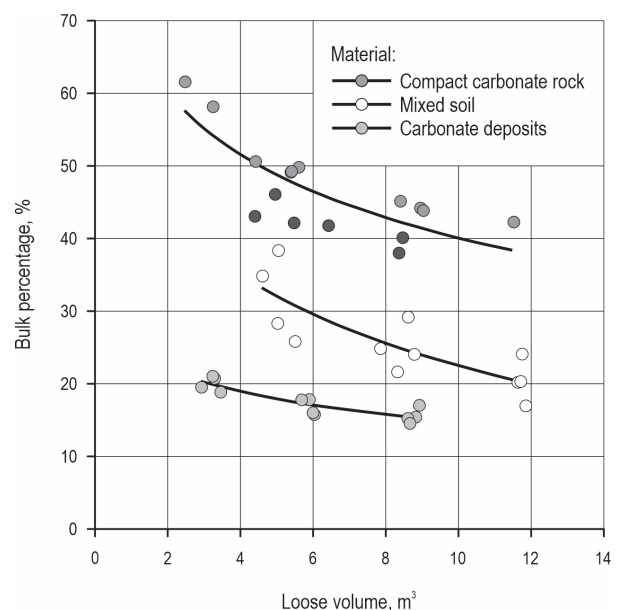

Fig. 4 Boxplots of bulk for three analysed materials

Fig. 5 Calculated bulk percentages for compact carbonate rock, mixed soil, and carbonate deposits; points for plots 5 and 6 (in black) indicate compact carbonate rock with greater porosity than in plots 1 to 4

4. Discussion

With modern remote sensing techniques, the volumes of excavated and loose materials were calculated for three most common materials used in forest road construction in Slovenia: compact carbonate rock, mixed soil, and carbonate deposits. A total of 3605 photographs were collected during 43 flights of the UAV (unmanned aerial vehicle). Their overall processing into point clouds took 64 hours and 44 minutes.

For each material investigated, the calculated bulk percentage decreases logarithmically with the volume excavated. The bulk percentage for compact carbonate rock varies from 60% on a 2.5 m^3 pile of loose material to 42% on a 11 m^3 pile, respectively. The existing research reported the corresponding percentages of 63% (Wilkinson 1997) and 66% (Peele 1961) for smaller quantities of loose material, without considering the consolidation of the material due to own weight (overburden stress). Our results for smaller piles are more similar to the above mentioned percentages than the ones for bigger piles.

In modern forest road construction, the excessive excavated material is not dumped over the road bank but trucked to the ladings or sections with excessive fills. The commonly reported unit is a fully loaded eight-wheeled truck, typically hauling 9 m^3 of loose material. Using the bulk factor, derived in laboratory conditions or from small piles, a significant increase in hauled quantities may appear if the trucks are counted. A typical forest road project on a mountainous terrain requires the allocation of approximately 4 m^3/m of forest road within the construction site. By using our expansion percentages for compact carbonate rocks instead of those described in literature, the investors might experience a 20% decrease in hauling costs. That does not mean that the percentages reported by Wilkinson (1997) or Peele (1961) are wrong, they just apply to smaller piles.

In our study, the percentages for compact carbonate rock for plots 5 and 6 were lower than those for the other plots due to a more fractured and porous original bedrock in plots other than plots 5 and 6 noted during the experiment. Ofoegbu et al. (2008) reported that bedrock porosity affects its fragmentation particularly when using a hydraulic hammer – a more porous bedrock will yield a larger share of smaller fractions. In our experiment, the excavator operator was required to produce grains of sizes up to 30 cm in all the plots. Although our image-based sieving curves (Fig. 3) for plots 5 and 6 are not significantly different

from others, all their calculated bulk percentages are below the fitted curve (Fig. 5). Since the image-based sieving analysis is an approximation of physical sieving, we suggest dry physical sieving in further research in order to validate the grain size and distribution effect on the bulk percentage. It has to be pointed out that the compact carbonate rock produced in the experiment was suitable for road bearing course. Consequently, the average bulk percentage derived will be used for similar purposes.

The bulk percentages determined for mixed soil, specifically dystric mixed soil, vary from 33% in a 5 m^3 pile to 20% in a 12 m^3 pile of loose material. The corresponding bulk percentages in other studies range from 20% to 30% (Engineering ToolBox 2009, and Peurifoy et al. 2006), emphasizing the need of target-oriented investigations for specific projects.

The bulk percentages determined for carbonate deposits vary from 20% in a 3 m^3 pile to 16% in a 12 m^3 pile of loose material. Referring to the corresponding values from other studies, we have to be careful regarding the influencing factors. Since there is no similar data, we compared our results to the values for sand and gravel. Peurifoy et al. (2006) indicate a gravel bulk percentage of 14%, Wilkinson (1997) a 15% bulk percentage for gravel and sand, and Engineering ToolBox (2009) state bulk percentages of 20% to 30%, respectively.

In plots with compact carbonate rock, we compared volumes calculated from total station and photogrammetric data. We found out that photogrammetric data are collected faster and that their accuracy is greater. By increasing the grid cell, the error of the volume increases, as was reported by Urbančič et al. (2015) for larger areas. For areas of 1000 m^2, we used a 2x2 cm cell grid. In this case, we must provide a sufficient density of the point cloud by choosing a suitable pixel size, photography overlapping, and UAV flight height. In our study, the distances between the points in the cloud were below 5 mm, hence a digital surface model with 1 cm cell grid could be created. Since the 1x1 cm cell grid does not significantly improve volume accuracy and triples the calculation time, we suggest a 2x2 cm grid cell for similar studies.

Finally, the coordinates for ground control points were determined on the Kamnica construction site by arithmetic means of triple independent measurements with GNSS RTK, while on the Kopiša and Pašni vrh sites, they were determined by the total station due to the lack of GPRS signal. The *RMSE* of all point clouds

for volume calculations were less than 0.008 m due to an adequate amount of ground control points suggested by Sanz-Ablanedo et al. (2018).

5. Conclusion

Based on the bulk percentages determined, we suggest material piles of approximately 9 m³ for loose material with the following average bulk factors: 1.42 for compact carbonate rock (s.e. 1.1), 1.20 for mixed soil (s.e. 1.5), and 1.15 for carbonate deposits (s.e. 0.5). The bulk factors for compact carbonate rock refer to uniformly graded material with the maximal grain of 30 cm in diameter. We can confirm hypothesis 1, that bulking factors differ over three common subsoils. Bulking factors from literature also differ from our calculated factors for compact carbonate rock and mixed soils for over 20% and can therefore confirm hypothesis 2.

The factors presented, determined by objective remote sensing methods, stand against subjectively assessed figures used daily in forest engineering in Slovenia. Since they comply well with past studies, we encourage further examination of the materials found in the forest infrastructure construction practice (e.g. sandstone, river deposits, magmatic rocks). The improved set of bulk factors provides a better evaluation of the materials moved on the jobsite and increases the reliability of the associated costs.

6. References

3Dsurvey. Available online: http://www.3dsurvey.si

Arango, C., Morales, C.A., 2015: Comparison between multicopter uav and total station for estimating stockpile volumes. Remote Sensing and Spatial Information Sciences (XL-1/W4): 131–135. https://doi.org/10.5194/isprsarchives-XL-1-W4-131-2015

Burch, D., 1997: Estimating Excavation. Craftsman Book: Carlsbad, CA, Center for Earthworks Engineering Research, 441 p.

Chopra, M.B., 1999: Investigation of Shrink and Swell Factors for Soils Used in FDOT Construction. Final Report: Orlando, Florida, University of Central Florida, Department of Civil and Environment Engineering: 194 p.

Church Horace, K., 1981: Excavation Handbook. McGraw-Hill: Pennsylvania Plaza, New York, 1024 p.

Crooks, A.R., 2013: Application of Shrinkage and Swelling factors on State Highway constuctions: Master thesis. Alabama USA, Graduate Faculty of Auburn University, 105 p.

CloudCompare (version 2.10.1) [GPL software]. Available online: http://www.cloudcompare.org/

Engineering ToolBox: Soil and Rock – Bulk Factors. Available online: https://www.engineeringtoolbox.com/soil-rock-bulking-factor-d_1557.html

ESRI, 2011: ArcGIS Desktop: Release 10.6. Redlands, CA, Environmental Systems Research Institute

Hugenholtz, C.H., Walker, J., Brown, O., Myshak, S., 2015: Earthwork Volumetrics with an Unmanned Aerial Vehicle and Softcopy Photogrammetry. Journal of Surveying Engineering 141(1): 06014003. https://doi.org/10.1061/(ASCE)SU.1943-5428.0000138

Kobal, M., Triplat, M., Kranjc, N., 2014: Pregled uporabe lasersekga skeniranja površja v gozdarstvu. Gozdarski vestnik: 72(5/6): 235–248.

Ofoegbu, G.I., Read, R.S., Ferrante, F., 2008: Bulking factor of rock for underground openings. Draft report prepared for U.S. Nuclear Regulatory Commission, U.S. Nuclear Regulatory Commission, 75 p.

Oštir, K., 2006: Daljinsko zaznavanje. Založba ZRC: Ljubljana, Inštitut za antropološke in prostorske študije., ZRC SAZU, 250 p.

Peurifoy, R.L., Schexnayder, C.J., Shapira, A., 2006: Construction Planning, Equipment and Methods, 7th ed.; McGraw-Hill Companies, Inc.: New York, NY, 396 p.

Peele, R., 1961: Mining Engineers' Handbook. 3rd Ed.; John Wiley & Sons: New York, 2775 p.

RStudio Team, 2015: RStudio: Integrated Development for R. Boston, MA, RStudio, Inc. Available online: http://www.rstudio.com/

Sanz-Ablanedo, E., Chandler, J.H., Rodríguez-Pérez, J.R., Ordóñez, C., 2018: Accuracy of Unmanned Aerial Vehicle (UAV) and SfM Photogrammetry Survey as a Function of the Number and Location of Ground Control Points. Remote Sensing 10(10): 1606. https://doi.org/10.3390/rs10101606 10 1606

Schenk, T., 2005: Introduction to photogrammetry. The Ohio State University, Department of Civil and Environmental Engineering and Geodetic Science, 95 p.

Split Engineering LLC, Split-Desktop Software. Available online: http://www.spliteng.com/products/split-desktop-software/

Strgar, I., 2004: Prostorninska masa in faktorji raztresenosti posameznih vrst nekovinskih mineralnih surovin v pridobivalnih prostorih v Republiki Sloveniji. Geologija 47(1): 119–121.

Telford, W.M., Geldart, L.P., Sheriff, R.E., Keys, D.A., 1976: Applied Geophysics. 2nd Ed.; Cambridge University Press: Cambridge, Massachusetts, 1608 p.

Urbančič, T., Grahor, V., Koler, B., 2015: Vpliv velikosti mrežne celice in metod interpolacij na izračunano prostornino. Geodetski vestnik 59(2): 231–245. https://dx.doi.org/10.15292/geodetski-vestnik.2015.02.231-245

Wilkinson, D., 1997: WWW Pages for Road Design. MEng final year project report. University of Durham: Durham, United Kingdom: School of University of Durham, 42 p.

Westerberg, S., Shiriaev, A., 2013: Virtual environment-based teleoperation of forestry machines: Designing future interaction methods. Journal of Human-Robot Interaction 2(3): 84–110. https://doi.org/10.5898/JHRI.2.3.Westerberg

Yilmaz, H.M., 2010: Close range photogrammetry in volume computing. Experimental Techniques 34(1): 48–54. https://doi.org/10.1111/j.1747-1567.2009.00476.x

Authors' addresses:

Jan Mihelič, MSc
jan.mihelic@sidg.si
Robert Robek, PhD
robert.robek@sidg.si
Slovenian State Forests Ltd.
Rožžna ulica 39
1330, Kočevje
SLOVENIA

Assoc. prof. Milan Kobal, PhD *
e-mail: milan.kobal@bf.uni-lj.si
University of Ljubljana
Biotehnical Faculty
Department of Forestry and Renewable Forest Resources
Večna pot 83
1000, Ljubljana
SLOVENIA

* Corresponding author